Available online at www.sciencedirect.com
ScienceDirect
C. R. Physique 8 (2007) 763–776
COMPTES RENDUS PHYSIQUE
http://france.elsevier.com/direct/COMREN/

Neutron scattering/Diffusion de neutrons

Neutron scattering on magnetic surfaces

Frédéric Ott

Laboratoire Léon Brillouin, CEA/CNRS UMR 12, Centre d'Etudes de Saclay, 91191 Gif-sur-Yvette cedex, France

Available online 19 November 2007

Abstract

During the early 1980s, advanced techniques for the deposition of ultra-thin metal films were developed. The combination of different types of materials gave rise to new physical phenomena such as the magnetic exchange coupling in superlattices or the exchange bias between ferro and anti-ferro layers. The field was very active because of the associated industrial applications in magnetic field sensors. New types of heterostructures combining magnetic oxides, insulating oxides or magnetic semiconductors are still being developed. Alongside the fabrication of these new meta-materials made of thin films stacking, polarized neutron reflectometry has emerged as a routine tool for the characterization of magnetic hetero-structures. In the recent years, the new developments of polarized reflectivity have been connected to the study of micro and nanostructures, especially micromagnetic structures in multilayers. The technique of off-specular scattering has been developed for the study of the roughness or the micromagnetism at a micrometric scale. For the study of nanometric structures, in the range below 100 nm, grazing incidence Small Angle Scattering is being considered. ***To cite this article: F. Ott, C. R. Physique 8 (2007).***

Résumé

Diffusion de neutrons sur des surfaces magnétiques. Dans les années 1980, les techniques de dépôt en films minces métalliques ont été développées. La combinaison de différents types de matériaux a conduit à l'apparition de nouveaux phénomènes tels que les couplages magnétiques dans les super-réseaux ou le couplage d'échange entre couches ferro et anti-ferromagnétiques. Le domaine a été très actif en raison des applications industrielles dans le domaine des capteurs magnétiques. De nouvelles hétéro-structures combinant des oxydes magnétiques, des isolants, des semi-conducteurs magnétiques, sont actuellement en développement. En parallèle de la synthèse de ces nouveaux méta-matériaux composés de sandwichs de couches minces, la réflectivité de neutrons polarisés a émergé comme un outil de caractérisation standard de ces systèmes. Dans la période plus récente, les nouveaux développements dans le domaine de la réflectivité de neutrons ont été connectés aux études de micro et de nano-structures, en particulier des structures micro-magnétiques. Des techniques dérivées de la réflectivité spéculaire comme la diffusion hors spéculaire ont été développées pour l'étude de la rugosité ou du micromagnétisme à l'échelle micrométrique. Pour l'étude de nanostructures dans une gamme de tailles caractéristiques inférieures à 100 nm, des techniques comme la diffusion aux petits angles en incidence rasante sont à l'étude. ***Pour citer cet article : F. Ott, C. R. Physique 8 (2007).***

Keywords: Neutron scattering; Magnetic surfaces

Mots-clés : Diffusion de neutrons ; Surfaces magnétiques

E-mail address: Frederic@cea.fr.

1631-0705/$ – see front matter
doi:10.1016/j.crhy.2007.09.002

1. Introduction

During the early 1980s, advanced techniques for the deposition of ultra-thin metal films were developed. This led to the fabrication of new artificial materials comprising of the stacking of different materials in thin sandwiches (hetero-structures). The combination of different types of materials gave rise to new physical phenomena. The first new phenomenon to be probed was the magnetic exchange coupling in superlattices (Fig. 1(a)). It appeared that magnetic layers separated by non-magnetic spacer layers can be magnetically coupled. The coupling can be either ferromagnetic, anti-ferromagnetic or more complex (quadratic or even helicoidal). The coupling can also change sign (from ferro to anti-ferro) as a function of the spacer layer thickness. Such phenomena were observed in rare-earth superlattices (Gd/Y, Dy/Y, Gd/Dy, Ho/Y [1]), transition metals super-lattices (Fe/Cr [2,3], Co/Cu [4], Fe/V [5], Co/Ru [6]), mixing of semiconductors and metals (Fe/Si [7], Fe/Ge [8]). The field is still open and new systems are being synthesized, especially with magnetic semiconducting materials (GaMnAs [9], EuS/PbS [10]).

These magnetic coupling phenomena are strongly connected to the Giant Magneto-Resistance effect [11]: depending on the orientation of the magnetization of the different layers in the hetero-structure, the resistivity of the system varies significantly. This has opened a new field of study which is now referred to as spintronics.

In the early 1990s, the phenomenon of exchange bias was revived. A ferromagnetic layer in contact with an anti-ferromagnetic material can be magnetically strongly coupled (Fig. 1(b)) [12,13]. The soft magnetic layer is thus strongly pinned along a well defined direction. This is presently used in most of the spintronics systems (Fig. 1(c)). The phenomenon is used in commercial devices, but is still not fully understood from a theoretical point of view. The origin of the coupling depends on the type of materials, their crystallinity, the fabrication process, ... [14].

In the late 1990s, it appeared that the performance of giant magneto-resistive systems could be enhanced by combining tunnel barriers and magnetic materials (using materials such as Fe_2O_3, Fe_3O_4, $CoFe_2O_4$, MgO, Al_2O_3). This field is very active and a number of phenomena still need to be understood. Electronic devices using magnetic tunnel junctions (such as Magnetic Random Access Memories) are about to be commercialized, but significant progress can still be made.

Besides the combination of well known materials, during the late 1990s, a wealth of new materials were synthesized (typically perovskites of the type $ABMnO_3$). The growth of these materials as epitaxial thin films was quickly mastered, following the experience acquired previously on oxide superconductors. These materials have properties ranging from colossal magneto-resistance to magneto-electric effects.

More recently, a new field has developed which is the search for new magnetic semiconductors. After the early studies of Eu-based magnetic semiconductors (EuO and EuS) in the 1970s, the field was dormant until GaMnAs magnetic semiconductors were synthesized in the middle of the 1990s. Since then, a number of new systems have been synthesized in order to find room temperature magnetic semiconductors. The discovery of a suitable material could boost the field of spintronics. These new materials range from diluted semiconductors to magnetically doped insulating oxide materials.

We can mention other types of studies such as the penetration of the magnetic flux in superconductor thin films [15], the exchange spring effect between soft and hard magnetic layers [16], the magnetism of ultra-thin films [17], proximity effects between magnetism and superconductivity [18], induced magnetism at interfaces (e.g. the magnetism induced in V in contact with Gd [19]), the super-anti-ferromagnetism (edge effects in Fe/Cr superlattices [20]).

In the recent years, the new developments of polarized neutron reflectivity have been connected to the study of micro and nanostructures especially micromagnetic structures in multilayers. These structures correspond to the formation of magnetic domains in the size range 100 nm–10 μm. This is motivated by the fact that the micromagnetic

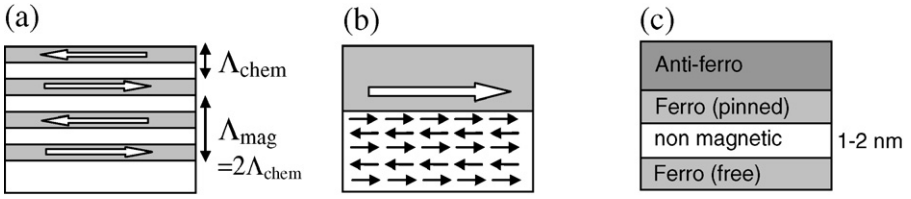

Fig. 1. (a) Exchanged coupled superlattice with an antiferromagnetic order. (b) Exchange bias between a ferromagnet and an anti-ferromagnet. (c) GMR system or magnetic tunnel junction.

structure plays a key role in the magnetic behavior of superlattices. It is also connected to the present trend which consists in patterning thin films into small structures so as to obtain a confinement not only in one direction but also in the thin film plane. Off-specular neutron scattering which is a technique derived from the specular, has been developed for the study of the roughness or the micromagnetism at a micrometric scale. For the study of nanometric structures (in the range below 100 nm), Grazing Incidence Small Angle Scattering is being considered.

In the following, we will present the different techniques of grazing incidence neutron scattering and then describe a few examples of measurements using these techniques.

2. Techniques

Our objective is to characterize magnetic surfaces and interfaces at the nanometric scale. This corresponds to very small volumes of matter, of the order of a few micrograms. Thus, it is necessary to develop surface scattering techniques. The use of neutron reflection at grazing incidence increases the neutron interaction with the sample surface and makes such experiments feasible. We will distinguish three scattering geometries (Fig. 2): specular reflection, scattering in the incidence plane (off-specular scattering) and scattering perpendicular to the incidence plane (Grazing Incidence SANS). These different scattering geometries probe different length scales ξ and directions in the sample surface. In a first part, we present the principle of specular reflectivity which probes the structure along the depth in the film (3 nm $< \xi <$ 100 nm). We will present the principle of the technique and some examples of applications on real multilayer systems. In a second part, we describe the principles of the off-specular scattering measurements which probe surface features at a micrometric scale (600 nm $< \xi <$ 60 μm). Finally, we discuss the extension of the small angle neutron scattering technique to the study of surfaces: Grazing Incidence SANS which probe surface features in the range 3 nm $< \xi <$ 100 nm. These different scattering geometries allow the study of a very wide range of length-scales ξ, from a few nm up to several μm.

2.1. Specular reflectivity

2.1.1. Principles

Neutrons can be reflected on surfaces in the same way as X-rays or electrons [21]. All the formalisms developed for X-ray reflectivity can be transposed for neutron reflectivity [22]. In a reflectivity geometry (Fig. 3(a)), the incidence angle θ_i on the surface is small (typically ranging from 0.5 to 5°). The reflection angle θ_r is the same as the incidence angle θ_i. As a consequence, the scattering wave-vector $\mathbf{Q}$ is perpendicular to the surface. The typical neutron wavelengths are in the range 2–20 Å. Thus the range of accessible scattering wave-vectors $\mathbf{Q} = \mathbf{k}_o - \mathbf{k}_i$ is 0.05–3 nm^{-1}. This corresponds in real space to typical length-scales between 2 and 100 nm. Neutron reflectivity is a technique

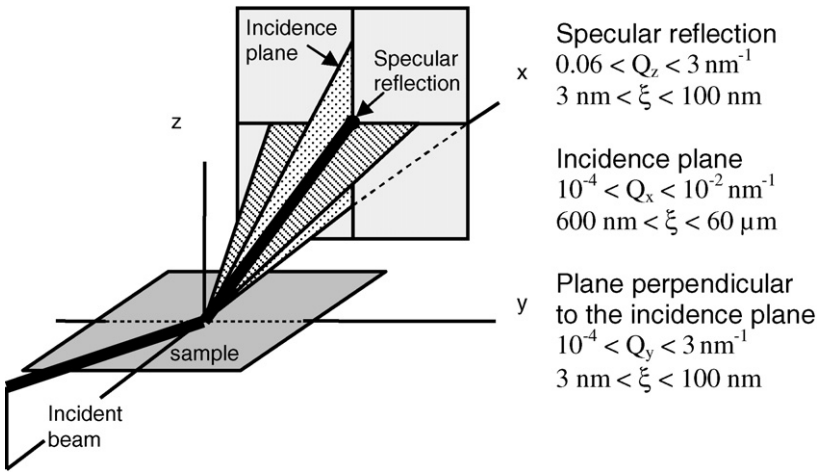

Fig. 2. The different surface scattering geometries. (Black line) specular reflectivity geometry; (dotted plane) off-specular scattering plane, corresponding to the incidence plane; (hashed plane) GISANS scattering plane, perpendicular to the incidence plane. These different scattering geometries probe a very wide range of length-scales and directions in the sample surface.

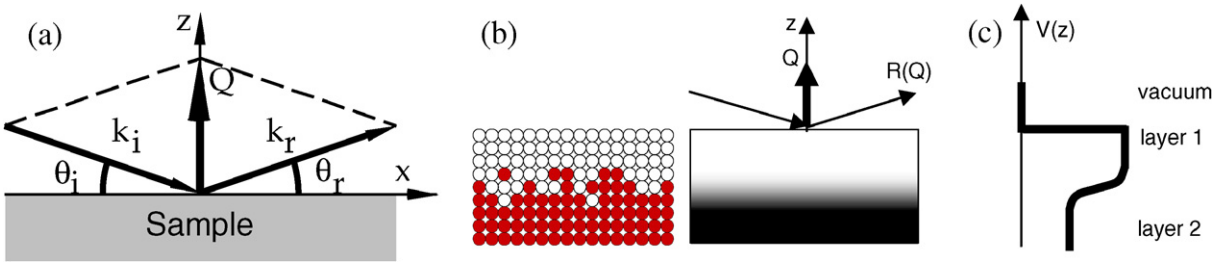

Fig. 3. (a) Specular reflectivity geometry. The reflection angle is equal to the incidence angle; the scattering wave-vector **Q** is perpendicular to the sample surface. (b) Interface between 2 layers. In the optical approximation, the interface is approximated as a continuous medium. (c) Reflection on a thin film deposited on a surface. The reflectivity measures the Fourier transform of the interaction potential $V(z)$.

Table 1
Nuclear and magnetic optical index $n = 1 - \delta \pm \delta_M$ for some materials at $\lambda = 0.4$ nm

Element	$\delta(10^{-6})$	$\delta_M(10^{-6})$	σ_a (barns)
Fe	20.45	11.7	2.56
Co	5.7	10.3	37.2
Ni	24	3.7	4.49
Gd	5.0	14.5	49 700
Si	5.3	–	0.17
Ti	−5	–	6.1
Al	6.11	–	0.23
SiO_2	10.1	–	

adapted for the study of thin films but does not probe structures at the atomic level. In a reflectivity geometry it is thus possible to use the 'optical approximation' [22] and to model the neutron interaction with the material as a continuous potential. The details of the atomic structure are smoothed out (Fig. 3(b)). The interaction potential V with a material is given by:

$$V = \frac{h^2}{2\pi m}\rho \quad \text{with } \rho = \sum_i N_i b_i \tag{1}$$

where h is the Planck constant and m is the neutron mass; ρ is called the 'scattering length density' and is the sum of the atomic density of the nuclei in the material N_i multiplied by their individual nuclear scattering lengths b_i.

In the case of a magnetic system, the interaction between the neutron spin and the material magnetization is of the form $V = -\boldsymbol{\mu} \cdot \mathbf{B}$ where $\boldsymbol{\mu}$ is the magnetic moment of the neutron and $\mathbf{B}$ is the magnetic induction inside the thin film.

In reflectivity geometry, the equivalent of a neutron 'optical index' can be derived from the Schrödinger equation [22]. Neglecting absorption, the value of this optical index is given by the following expression:

$$n^{\pm} \approx 1 - \delta \pm \delta_M = 1 - \frac{\lambda^2}{2\pi}\rho \pm \frac{m\lambda^2}{h^2}\mu.B \tag{2}$$

where δ is the nuclear contribution to the optical index, and δ_M is the magnetic contribution to the optical index, the sign of the magnetic contribution depends on the relative orientation of the neutron spin with respect to the magnetization (parallel or anti-parallel). Table 1 gives values of optical indexes for some typical materials. One should notice that the magnetic optical index is of the same order of magnitude as the nuclear optical index. The use of polarized neutrons permits to measure both optical indexes n^+ and n^- and thus to obtain detailed information about the magnetic structure of the sample.

In a specular reflectivity measurement, the most important assumption is that the system is invariant in translation in the thin film plane, that is, there are no inhomogeneities along the film surface. Thus the interaction potential V is assumed to be only a function of the depth z in the multilayer system (Fig. 3(c)). In a first approximation, the specular reflectivity measures the Fourier transform of the optical index profile $n(z)$.

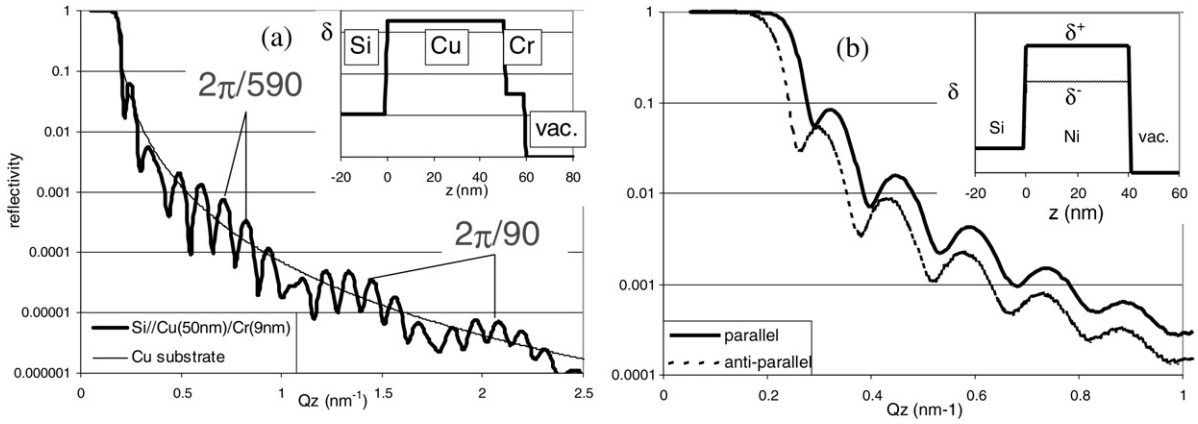

Fig. 4. (a) Reflectivity on a multilayer system Si//Cu(50 nm)/Cr(9 nm). The short period oscillations are characteristic of the total thickness of the layer (59 nm); the long range modulation is characteristic of the thin Cr layer (9 nm). (Insert) optical index profile as a function of the depth in the film. (b) Reflectivity of a magnetic film Si//Ni(40 nm). The reflectivity depends on the relative orientation of the neutron spin with respect to the magnetization. (Insert) optical index profile for both neutron polarizations (parallel and anti-parallel).

However, at low incidence angles, there is total reflection up to a critical wave-vector $Q_c = 4\sqrt{\pi\rho}$ and thus the Born approximation is not valid at small scattering wave-vectors. The Born approximation can be applied only above a scattering wave-vector of about $3Q_c$. Below this limit, one must solve the Schrödinger equation and perform a full dynamical calculation. The detailed theoretical treatment of the polarized reflectivity can be found in [22–26]. Fig. 4(a) presents the situation of the reflection of a neutron beam on a multilayer Si//Cu/Cr: above the critical wave-vector of total reflection, the reflected intensity decreases as $1/Q^4$. Modulations of the reflected intensities are observed. They correspond to constructive and destructive interferences of the neutron waves scattered by the different interfaces of the multilayer system. These oscillations are called Kiessig fringes. Their pattern is characteristic of the multilayer system. Fig. 4(b) presents the situation of a magnetic thin film on a substrate. In this case, the optical index depends on the relative orientation of the neutron spin with respect to the thin film magnetization. The measured reflectivity is very different for neutrons incident with a spin parallel to the magnetization (optical index $n^+ = 1 - \delta - \delta^+$) and for neutrons incident with a spin anti-parallel to the magnetization (optical index $n^- = 1 - \delta + \delta^-$).

The measure of the reflectivity probes the profile of optical index $n(z)$ along the normal (Oz) to the thin film system. Numerical models are then used to reconstruct the thickness of the different layers of the system as well as their individual scattering length densities which are characteristic of their chemical composition. Inter-diffusion and roughness at interfaces can be quantified with more detailed models. In the case of magnetic systems, information on the amplitude and the direction of the magnetization of the different layers can be obtained using polarized neutron reflectivity. One should note that polarized reflectivity is sensitive to the induction in the thin films: no difference is made between the spin and orbital magnetic moments. In practice, it is possible to measure 4 cross-sections in a polarized reflectivity experiment: 2 non-spin-flip cross-sections, R^{++} (resp. R^{--}), corresponding to the number of incoming 'up' (resp. 'down') neutrons reflected with an 'up' (resp. 'down') polarization; 2 spin-flip cross-sections, $R^{+-} = R^{-+}$, corresponding to the number of neutrons experiencing a spin-flip during the reflection on the sample. In a first approximation, the non-spin-flip cross-sections probe the components of the magnetization which are parallel to the applied field; the spin-flip cross-sections are sensitive to the component of the magnetization perpendicular to the applied field. Combining this information it is possible to reconstruct the magnetization direction and amplitude along the depth of the film. The depth resolution is of the order of 2–3 nm in simple systems. Polarized reflectivity is a surface technique and thus is not sensitive to paramagnetic or diamagnetic contributions from the substrate. There is no absorption. There are no phenomenological parameters. The data are 'naturally' normalized. All these characteristics make neutron reflectivity data easy to model and interpret.

In the following, we shall restrict ourselves to 2 examples illustrating some of the possibilities offered by polarized reflectivity: super-lattices and single thin films. For other examples, the interested reader should refer to the following recent reviews [27–31].

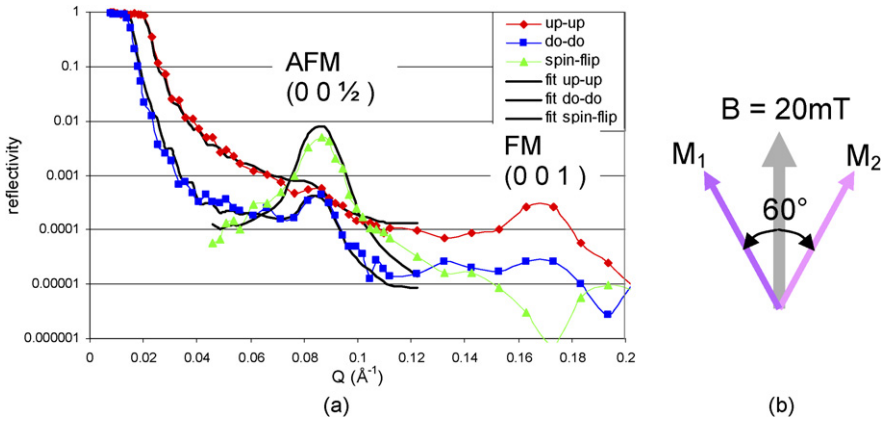

Fig. 5. (a) Reflectivity of a [Fe(2.4)/Si(1.2)]$_n$ multilayer measured at 5 K. (b) Configuration of the magnetic moments in 2 adjacent Fe layers.

2.1.2. Super-lattices

In multilayers where magnetic layers are separated by a non-magnetic spacer, different types of coupling can appear: ferromagnetic, anti-ferromagnetic or quadratic (at 90°). The observation of magnetic coupling has been observed in a wide range of heterostructures. The most thoroughly studied system is the metallic system Fe/Cr. Pioneering polarized neutron reflectometry studies have been performed on this system [32]. Though the origin of the magnetic coupling is well understood in metallic hetero-structures [33], the exact origin of the ordering in structures combining semiconductors or even insulators is still unclear.

We present here the example of GaAs//[Fe(2.4 nm)Si(1.2 nm)]$_{20}$ multilayers produced by K. Fronc [6]. The reflectivity of the system at low temperature is presented on Fig. 5. One observes a diffraction peak [0 0 1] corresponding to the chemical modulation at the position $Q = 0.17$ nm^{-1}. The magnetic contrast corresponds to the amplitude of the magnetization along the applied field. More interestingly, another diffraction peak is observed at the position [0 0 1/2]. This is a peak of purely magnetic origin. It indicates that an anti-ferromagnetic coupling exists between adjacent Fe layers. The striking feature is that the spin-flip signal is dominant. A numerical modeling suggests that the magnetizations of adjacent Fe layers make an angle of 30° with respect to the applied field (Fig. 5(b)). An analysis of the chemical profile reveals that the system cannot be described as a perfect stacking of Fe and Si layers, a strong interdiffusion exists and none of the layers are pure. The question of the origin of the coupling remains unclear.

The studies of the magnetic coupling in magnetic superlattices are still numerous: in 'all metal' superlattices we can mention Pd/Fe [34], Heussler alloys [35,36], U/Fe [37]; in semiconductors Fe/Ge [38]; in rare-earths $DyFe_2/YFe_2$ [39], Ho/Y [40]; in metal/oxide layers Co/Al_2O_3 [41].

2.1.3. Magnetic single layers

Even though most of the studies are performed on super-lattices (usually for intensity reasons), the magnetization of very thin systems can also be probed. The advantage of studying simple systems is that much more detailed information can be obtained since the signal is not blurred by roughness or thickness fluctuations. We present here the example of the study of a coupled FeCo/Mn/FeCo tri-layer system [42]. The structure of the sample is shown on Fig. 6(a). The 'active' region is formed by the layers FeCo/Mn/FeCo. The Ag layer is used to promote an epitaxial growth of the system. The Au layer is a simple protective capping. The system presented is $Fe_{0.5}Co_{0.5}$/Mn(8 Å)/$Fe_{0.5}Co_{0.5}$. The specificity of this system is that the magnetic couplings between Fe and Mn, and Co and Mn are of opposite sign. Ab initio calculation predicted that in such a system, contrary to a pure Fe/Mn interface, a complex magnetic behavior of the Mn layer arises. A first measurement was performed in a saturating field (not shown). A numerical modeling of the data shows that the magnetic moment in the $Fe_{0.5}Co_{0.5}$ layers is 2.4 μ_B/atom (as in bulk materials). A net magnetic moment of 0.8 μ_B/atom in Mn is also observed. This induced magnetization in the Mn layer was theoretically predicted for FeCo alloys by the abinitio calculations. In similar systems without Co, no magnetic moment is observed in the Mn layer.

The applied field was then decreased down to 1.2 mT. The reflectivity was remeasured. In these conditions a large spin-flip signal is observed (Fig. 6(b)). The reflectivity data was fitted by letting the magnetization directions vary. The

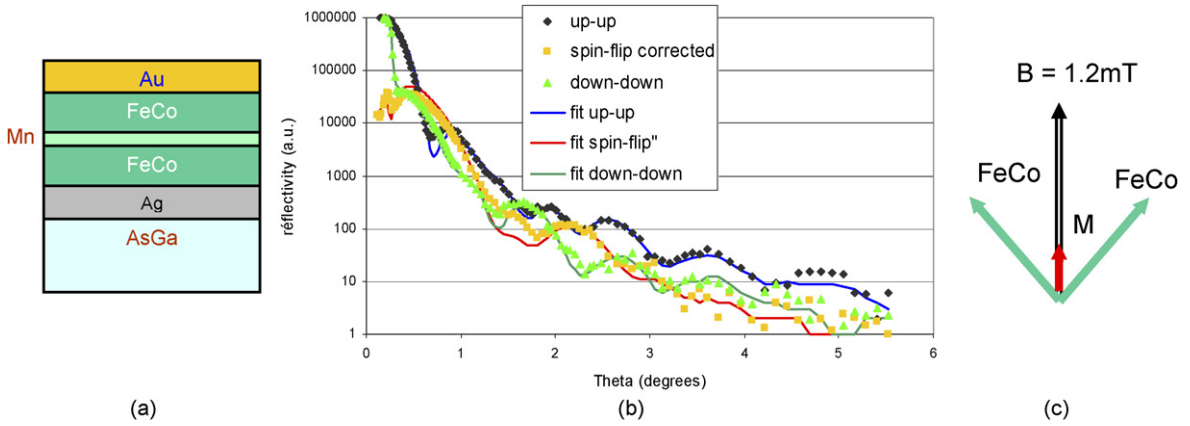

Fig. 6. (a) Trilayer system. (b) Reflectivity in the remanent state. (c) Magnetic configuration as deduced from the fit.

best adjustment was obtained when the magnetization of the layers make an angle of 45° with respect to the applied field. The two magnetic layers make an angle of 90°, we have a quadratic coupling.

Polarized neutron reflectivity has also been used to probe the magnetism of individual thin films such as oxide layers (manganites [43,44] or Fe_3O_4 [45]) or Fe ultra thin films deposited on various substrates [46–48].

2.1.4. Exchange bias—spin-valves

The magnetic thin film system which has enjoyed the most popularity until now is the spin-valve. It consists of a stack of two magnetic layers separated by a non-magnetic spacer. The electrical resistance of the system depends on the relative orientation of the magnetizations. In industrial systems, one of the magnetic layers is pinned by a coupling with an anti-ferromagnetic material through the so-called exchange-bias mechanism. The materials which are used in such structures are numerous: Co, Fe, Ni, NiFe, Fe_3O_4, $CoFe_2O_4$, $LaSrMnO_3$, ... for ferromagnetic layers; Cu, Cr, V, Al_2O_3, HfO_2, $SrTiO_3$, ... for the spacer layers; FeMn, IrMn, CoO, Co/Ru/Co, Fe_2O_3, NiO, $BiFeO_3$, ... for the antiferromagnetic exchange bias layer.

Such spin valve systems have been extensively characterized [49–52] and are now well understood. However, the microscopic understanding of exchange bias has been a long standing problem for decades now. A wealth of literature is being produced on numerous and various systems [53–57]. It appears that the exchange bias mechanism combines very subtle effects. The reversal process of the coupled magnetic layer has been studied in detail. Since the origin of the phenomenon is often linked to micromagnetic problems, reflectivity studies are often complemented with off-specular scattering which probes the underlying micromagnetic structures. This technique is described in the following.

2.2. Off-specular scattering

In the case of the specular reflectivity, the scattering vector **Q** is perpendicular to the sample surface and thus one probes the structure of the sample along its depth only. All the structures in the thin film plane are averaged out. This information is sufficient as long as there is no formation of magnetic domains in the structure and that it can be assumed that the magnetization is homogeneous in each layer of the system. If this is not the case, by slightly modifying the scattering geometry, that is, by introducing a small in-plane component of the scattering wavevector (Fig. 7) it is possible to probe in-plane structures. The specificity of the off-specular reflectivity geometry is that the in-plane component Q_x of the scattering vector is very small, of the order of 0.1–10 μm^{-1}. In this scattering geometry, one will be mostly sensitive to in-plane lateral structures with characteristic sizes ranging from 50 μm down to 0.5 μm. The upper limit is set by the resolution of the spectrometer and the size of the direct beam. The lower limit is set by the available neutron flux. These sizes correspond to typical sizes of micro-magnetic domain structures. Thus magnetic off-specular scattering is mostly used to probe such problems. These measurements are usually performed by using a position sensitive detector after the sample and measuring the scattering on the detector as a function of the incidence angle.

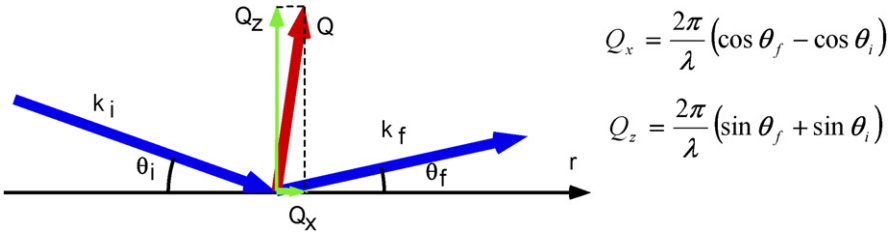

Fig. 7. Off-specular scattering geometry. The scattering vector **Q** is not perpendicular to the thin film plane anymore. There is a small component in the thin film plane.

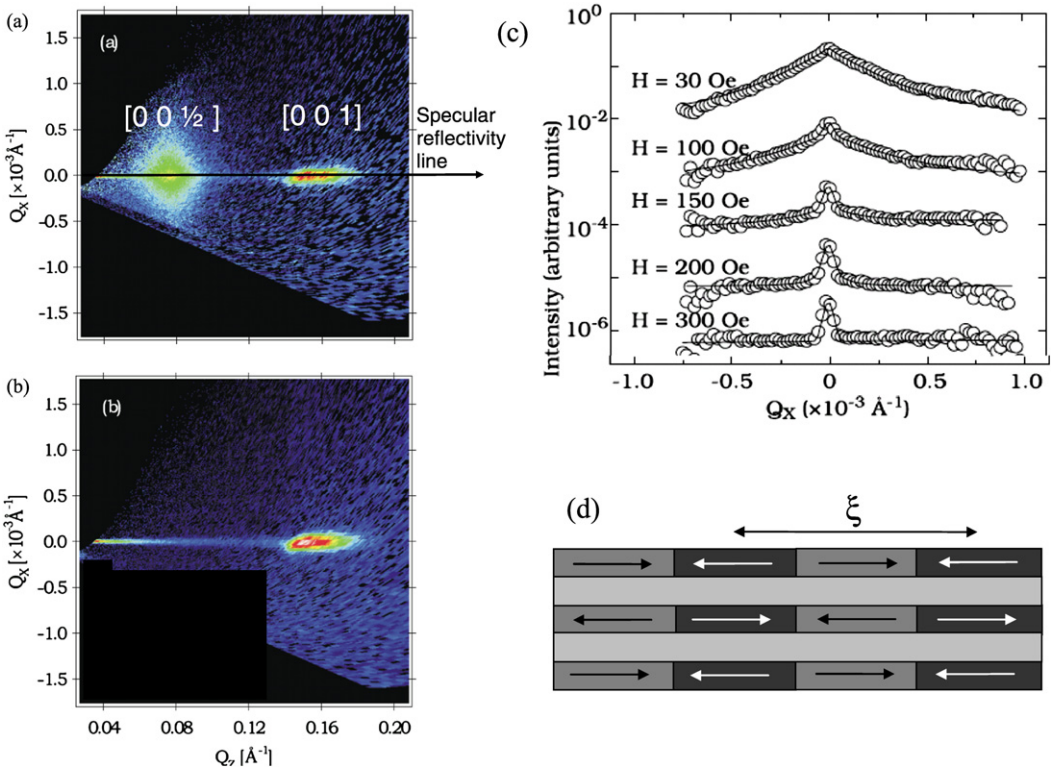

Fig. 8. $[Co(2\ nm)/Cu(2\ nm)]_{50}$ multilayers (adapted from Langridge et al. [4]). (a) Diffuse neutron scattering at $H = 0$. One observes a strong diffuse signal at the AF position. (b) Diffuse scattering in a saturating field. The AF peak has disappeared. (c) Evolution of the AF peak as a function of the applied field (cut along $Q_z = 0.75\ nm^{-1}$). (d) Magnetic coupling between the layers. ξ is the lateral correlation length between magnetic domains. The Co layers are locally coupled AF but there is a strong disorder within each Co layer.

The pioneering work in the field of off-specular scattering was presented in the early 1990s [58]. For flux reasons, until now, most of these studies have been performed on multilayer systems. Fig. 8 presents an example of the off-specular scattering from a $[Co/Cu]_{50}$ multilayer.

The diffuse signal has been measured as a function of Q_x and Q_z. On Fig. 8(a) and (b), one observes the structural correlation peak [0 0 1] corresponding to the chemical periodicity. At remanence, a strong diffuse scattering peak is observed at the position [0 0 1/2]. Since the magnetic diffuse scattering is localized around the position [0 0 1/2], it is possible to say that the Co layers are globally anti-ferromagnetically coupled along the thickness of the layer. However, since there is a strong diffuse scattering, it is also possible to say that there exists a significant magnetic disorder in the plane of the Co layers. The width of the diffuse scattering peak around the position [0 0 1/2] (Fig. 8(c)) is inversely proportional to the magnetic domain size and gives an estimate of its mean value which ranges from 1 μm at remanence (30 G) up to 6 μm at 250 G.

Magnetic off-specular scattering has been mostly used to probe the sizes of magnetic domains in multilayers. Detailed quantitative analysis of the magnetic off-specular scattering can be performed [20]. The effect of the micromagnetic structure can then be correlated with other properties such as the magneto-crystalline anisotropy (in Fe/Cr superlattice [59]) or the magneto-resistive effect (in Fe/Cr [60] or Co/Cu [61] superlattices). The formation of micromagnetic structures is very important with respect to the transport properties in magnetic sensors. The signal-to-noise ratio of Giant Magneto Resistive systems is very sensitive to the micromagnetic structure [43]. Off-specular studies are also used to complement studies on exchange bias systems: Co/CoO [62], $Ir_{20}Mn_{80}/Co_{80}Fe_{20}$ [63]. Off-specular scattering has also been used to study the problem of the reversal process in neutron polarizing super-mirrors [64]. In some special cases, it has been shown that it is also possible to probe single interfaces (Fe/Cr/Fe trilayer [65] or waveguide structures [66]).

The trend in nanosciences is shifting from continuous thin films to in-plane nanostructures. These nanostructures can be obtained by patterning or by self-organization [67–70]. In a number of studies, the influence of patterning on the exchange bias has been probed [71–74]. These studies are of interest when the magnetic heterostructures are to be integrated in large scale micro-circuits (typically for Magnetic RAMs).

2.3. Grazing incidence scattering

Since nanosciences are aiming at smaller scales (well below 1 μm), off-specular scattering will reach its limits since it is limited to probing rather large correlation lengths ($\xi > 500$ nm). This is why surface scattering has been extended to the SANS geometry. In this case, one looks at the scattering in the plane perpendicular to the incidence plane (Fig. 1, hashed plane). The scattering wavevector is given by $Q_x = k_0.\Delta\theta_y$ and is in a range comparable to the scattering wavevectors in SANS experiments: $10^{-4} < Q_y < 3\ \text{nm}^{-1}$. This corresponds to correlation lengths ξ ranging from 3 to 100 nm.

We present here the first example of a Grazing Incidence SANS experiment on a magnetic thin film [75]. FePt thin film layers self organize in magnetic stripe domains (Fig. 9(a)). The stripes are almost perfectly ordered as a periodic pattern with a period of about 100 nm. In order to study in-depth this magnetic pattern, a Grazing incidence SANS experiment was performed on the spectrometer PAPYRUS at the LLB. The neutron beam was sent at grazing incidence ($\theta_{\text{in}} = 0.7°$) on the layer, the magnetic domains being parallel to the incidence plane (Fig. 9(a)). Diffraction from the magnetic domains can be observed. Fig. 9(b) details the different contributions of the Grazing Incidence SANS signal. An integration at fixed Q_z has been performed and is presented on Fig. 9(c). Three diffraction orders can be observed (the second order being extinct). In order to model the system, it is necessary to take into account the Néel caps between the magnetic stripes as well as the magnetic stray fields (Fig. 9(d)) [76].

Other systems with stripe domains have been studied (ex. Fe/FeN [77]). Systems of magnetic Fe nanodots have also been observed using Grazing Incidence SANS [78].

Compared to Magnetic Force Microscopy, which is a direct space probe, the technique permits to probe buried layers and to obtain quantitative information about the magnetization. Force microscopy only gives surface information and no quantitative information. The other advantage is that it is also possible to set-up complex sample environments (furnace–cryostat–high magnetic fields). The strong limitation is however that presently the neutron flux is rather low and long counting times are required. As dedicated instruments will be developed the situation will improve.

2.4. Diffraction

In the previous examples, we discussed small angle scattering experiments on thin films. In this scattering geometry, it is not possible to access to atomic details of the systems. In thin films, the volume of magnetic matter is very small but nevertheless, diffraction experiments can be performed owing to the good performances of modern neutron spectrometers. Though the Grazing Incidence geometry can be used [79], in practice, it proves much easier to use a direct diffraction geometry which permits scanning the whole **Q** space. In a direct scattering geometry, it is possible to probe epitaxial thin films with thicknesses down to 10 nm.

In the example presented on Fig. 10, the first order magnetic transition in a MnAs film (100 nm thick) between the magnetic phase α of MnAs and the paramagnetic β phase was followed by neutron diffraction. One can observe that both phases coexist over a wide temperature range (~ 70 K) and that the behavior of epitaxial films is very different compared to bulk systems.

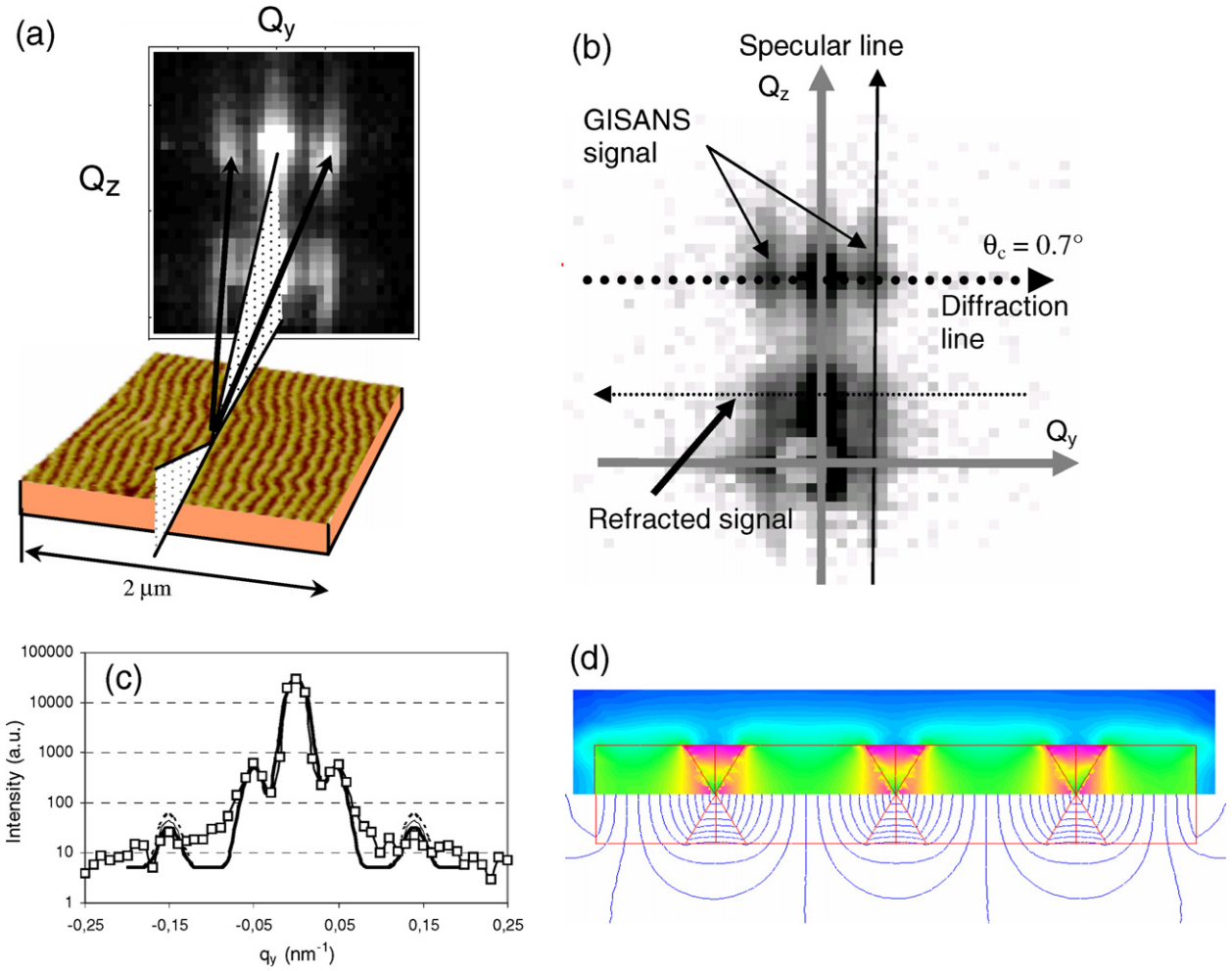

Fig. 9. GISANS signal from a magnetic domains nanostructure. (a) Magnetic Force Microscopy image of the magnetic domains and scattering geometry. (b) GISANS signal on the detector for $\theta_{in} = 0.7°$. (c) GISANS signal at constant Q_z. (d) Distribution of the magnetic induction in the thin films.

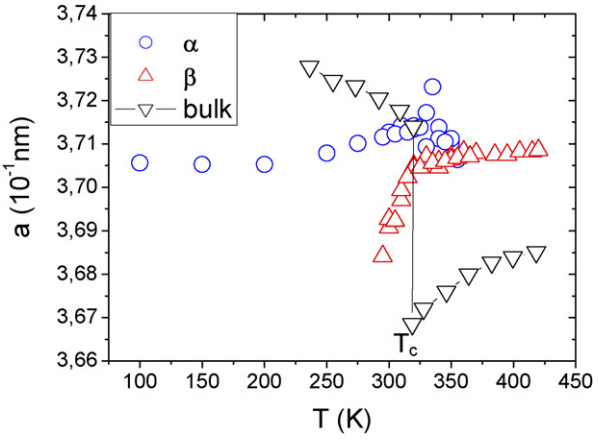

Fig. 10. Evolution of the lattice parameters a of an epitaxial MnAs thin film [80] as a function of the temperature. (Circles) α-phase, (triangles) β-phase, (diamonds) in a bulk sample. One can see that in the thin film, the α and β phases coexist over 70 K around the transition temperature.

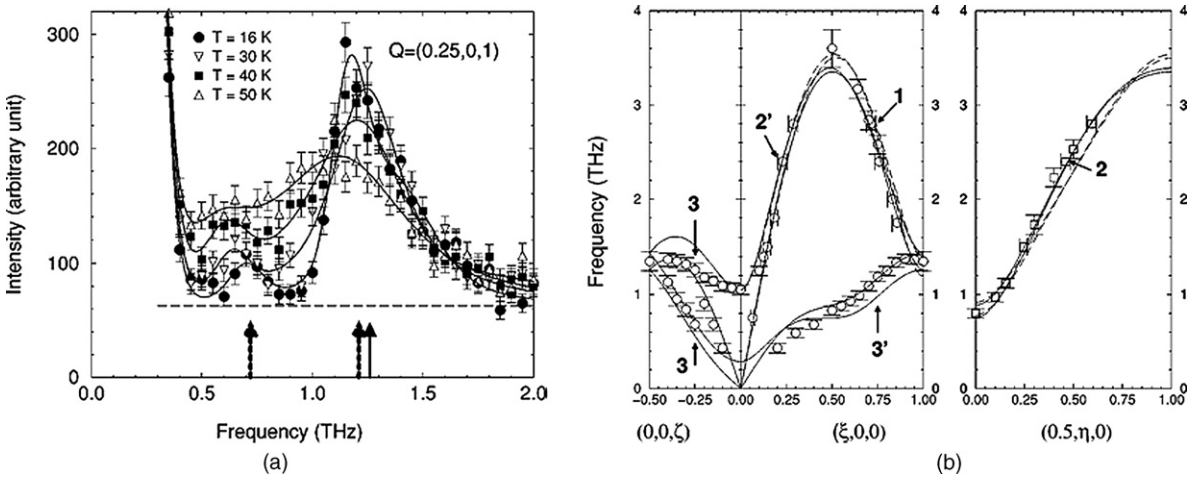

Fig. 11. (a) Temperature dependence of the spin-wave modes in a MnTe epitaxial film. (b) Spin wave dispersion at $T = 15$ K (adapted from [85]).

A number of diffraction studies have also been performed on epitaxial RE thin films [81–83] in which the large magnetization of rare earths helps performing precise measurements.

2.5. Inelastic scattering

Attempts have been made to perform inelastic measurements on magnetic thin films. They have been restricted to very specific samples. These inelastic measurements were limited to the study of rather thick films (∼1 μm) and materials with large magnetic moments (Dy [84] and Mn [85], Fig. 11). Other attempts have been made to study the dynamics in the GHz range (magneto static excitations) [86] but were not successful. Presently, the study of inelastic scattering in thin films is limited to feasibility studies and is not a mainstream technique.

3. Conclusion—future

3.1. Neutron—X-ray comparison

In the last decade, great efforts have been made to apply X-ray scattering to the study of the magnetism of thin films. The high flux available on the synchrotron sources compensates for the weak magnetic interaction of X-rays. In this paragraph we want to underline the strengths and weaknesses of the different scattering techniques. Neutron reflectivity has the following characteristics:

+ It is a direct quantitative probe of the magnetization. The data processing is very simple and quantitative. It is straightforward to obtain the magnetization profile (amplitude and direction) in a thin film system;
+ Complex sample environments are available (very low temperatures, high temperatures, high magnetic fields);
+ It is possible to probe buried layers (protective capping can be used). The corollary is that it is possible to probe complex systems consisting of several layers. It is not necessary to design the system specifically for the scattering experiment;
– The flux is low and several hours of measurements are required for each sample and experimental conditions;
– Neutrons have a weak chemical sensitivity and resonant techniques or spectroscopic techniques do not exist;
– It is not possible to distinguish the spin and orbital moments;
– Measuring times are long. Dynamics can be probed only down to ∼10 μs in stroboscopic mode.

The techniques of magnetic X-ray scattering (X-ray dichroism; resonant X-ray reflectivity; X-ray imaging) have the following advantages/disadvantages:

+ High flux;
+ Chemical sensitivity;

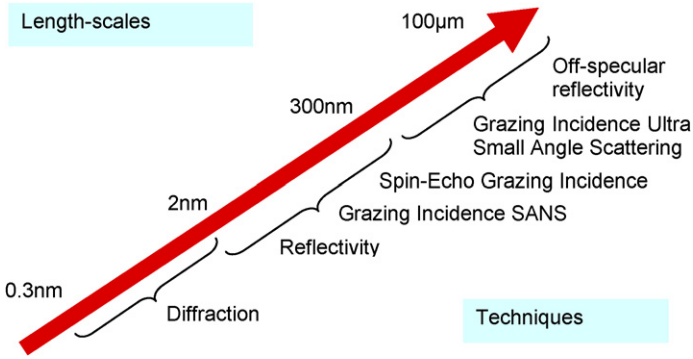

Fig. 12. Correlation lengths and suitable scattering techniques.

+ High speed dynamics;
+ Imaging possibilities (sub-µm);
– The data processing is very complex because the magnetic interaction is tensorial. Quantitative data are difficult to extract on complex materials;
– It is difficult to setup complex sample environments;
– It is difficult to probe buried layers;
– No vector magnetometry.

3.2. Future evolutions

A very large range of correlation lengths in thin film systems can now be probed using neutron surface scattering techniques.

A wide set of techniques are available (Fig. 12): specular neutron reflectivity which is operated routinely, off-specular scattering which is easily performed but requires heavy data processing, Grazing Incidence SANS which is still in development, and diffraction on thin films which in the case of good quality systems is feasible. For the foreseeable future, inelastic experiments on thin films will be restricted to very specific systems.

Presently, an effort is made in order to increase the flux on neutron reflectometers. Flux gains ranging from 10 to 100 can reasonably be expected in the next decade through the implementation of new types of neutron reflectometers. Quantitative gains in the measuring time and in the minimum sample size will be achieved. However, it is not yet clear if qualitative gains (new types of measurements besides the ones presented in this communication) are possible.

During these last 2 decades, polarized neutron reflectometry has proved to be a useful tool for the topics discussed above. In the early studies of magnetic superlattices, new types of magnetic orders were directly and unambiguously probed. Since then it has systematically been used for the study of magnetic thin films heterostructures. It is even used to characterize industrial systems. It is now complemented by new tools using the magnetic sensitivity of X-rays: magnetic X-ray diffraction or reflectivity and X-ray dichroism.

References

[1] C.F. Majkrzak, et al., J. Appl. Phys. 63 (1988) 3447–3452;
C.F. Majkrzak, et al., Phys. Rev. Lett. 56 (1986) 2700–2703.
[2] P. Grünberg, et al., Phys. Rev. Lett. 57 (1986) 2442.
[3] A. Schreyer, et al., Phys. Rev. Lett. 79 (1997) 4914–4917.
[4] S. Langridge, et al., Phys. Rev. Lett. 85 (2000) 4964–4967.
[5] B. Hjörvasson, et al., Phys. Rev. Lett. 79 (1997) 901.
[6] Y.Y. Huang, G.P. Felcher, S.S.P. Parkin, J. Magn. Magn. Mater. 99 (1991) 31–38.
[7] W. Szuszkiewicz, et al., J. Supercond. 16 (2003) 205–208.
[8] S. Singh, et al., J. Appl. Phys. 101 (2007), Art. No. 033913.
[9] H. Kepa, et al., Phys. Rev. B 64 (2001) 121302;
W. Szuszkiewicz, et al., J. Supercond. 16 (1) (2003) 209–212.
[10] H. Kepa, et al., Europhys. Lett. 56 (2001) 54–60.

[11] M.N. Baibich, et al., Phys. Rev. Lett. 61 (1988) 2472.
[12] S.G.E. te Velthuis, et al., Phys. Rev. Lett. 89 (2002) 127203;
S.G.E. te Velthuis, et al., J. Appl. Phys. 87 (2000) 5046;
S.G.E. te Velthuis, et al., Appl. Phys. Lett. 75 (1999) 4174–4176.
[13] F. Radu, et al., J. Magn. Magn. Mater. 240 (2002) 251–253;
F. Radu, et al., Phys. Rev. B 67 (2003) 134409.
[14] J. Noguès, et al., J. Magn. Magn. Mater. 192 (1999) 203–232;
M.R. Fitzsimmons, et al., Phys. Rev. Lett. 84 (2000) 3986–3989;
M. Gierlings, et al., Phys. Rev. B 65 (2002) 092407/1–4.
[15] V. Lauter-Pasyuk, et al., Physica B 248 (1998) 166–170.
[16] K.V. O'Donovan, et al., Phys. Rev. Lett. 88 (2002) 067201/1–4.
[17] D. Haskel, et al., Phys. Rev. Lett. 87 (2001) 207201/1–4;
V. Leiner, et al., Physica B 283 (2000) 167–170.
[18] J. Stahn, et al., Phys. Rev. B 71 (2005) 140509;
J. Chakhalian, et al., Nature Phys. 2 (4) (April 2006) 244–248.
[19] L.T. Baczewski, et al., Phys. Rev. B 74 (2006) 075417.
[20] V. Lauter-Pasyuk, et al., Phys. Rev. Lett. 89 (2002) 167203.
[21] J. Lekner, Theory of Reflection of Electromagnetic and Particle Waves, Martinus Nijhoff, Dordrecht, 1987.
[22] C. Fermon, F. Ott, A. Menelle, Neutron reflectivity, in: J. Daillant, A. Gibaud (Eds.), X-Ray and Neutron Reflectivity: Principles and Applications, in: Springer Lecture Notes in Physics, Springer, Berlin, 1999, p. 163;
F. de Bergevin, in: J. Daillant, A. Gibaud (Eds.), X-Ray and Neutron Reflectivity: Principles and Applications, in: Springer Lecture Notes in Physics, Springer, Berlin, 1999, p. 3.
[23] G.P. Felcher, et al., Rev. Sci. Instrum. 58 (1987) 609–619.
[24] S.J. Blundell, J.A.C. Bland, Phys. Rev. B 46 (1992) 3391–3400.
[25] C. Fermon, C. Miramond, F. Ott, G. Saux, J. Neutron Res. 4 (1996) 251.
[26] Z. Pleshanov, Physica B 94 (1994) 233–243.
[27] C.F. Majkrzak, Physica B 221 (1996) 342–356.
[28] H. Zabel, R. Siebrecht, A. Schreyer, Physica B 276–278 (2000) 17–21.
[29] H. Zabel, K. Theis-Brohl, J. Phys. Condens. Matter 15 (2003) S505–S517.
[30] G.P. Felcher, J. Appl. Phys. 87 (2000) 5431–5436;
G.P. Felcher, Physica B 267–268 (1999) 154–161.
[31] M.R. Fitzsimmons, et al., J. Magn. Magn. Mater. 271 (2004) 103–146.
[32] J.A.C. Bland, et al., J. Magn. Magn. Mater. 93 (1991) 513–522;
A. Schreyer, et al., Europhys. Lett. 32 (1995) 595–600.
[33] D.E. Bürgler, P. Grünberg, S.O. Demokritov, M.T. Johnson, Interlayer exchange coupling in layered magnetic structures, in: K.H.J. Buschow (Ed.), Handbook of Magnetic Materials, vol. 13, Amsterdam, Elsevier, 2001, p. 1.
[34] L. Cheng, et al., Phys. Rev. B 69 (2004) 5.
[35] A. Bergmann, et al., Phys. Rev. B 72 (2005) 12.
[36] M. Vadala, et al., J Phys. D Appl. Phys. 40 (2007) 1289.
[37] A.M. Beesley, et al., J. Phys. Condens. Matter 16 (2004) 8507.
[38] S. Singh, et al., Electrochem. Solid State Lett. 9 (2006) J5.
[39] M.R. Fitzsimmons, et al., Phys. Rev. B 73 (2006) 134413.
[40] V. Leiner, M. Ay, H. Zabel, Phys. Rev. B 70 (2004) 1.
[41] S. Bedanta, et al., Phys. Rev. B 74 (2006) 5.
[42] S. Nerger, et al., Physica B 297 (2001) 185–188.
[43] F. Ott, et al., J. Mag. Mag. Mater. 211 (2000) 200–205.
[44] R.P. Borges, et al., J. Appl. Phys. 89 (2001) 3868–3873.
[45] J.-B. Moussy, et al., Phys. Rev. B 70 (2004) 174448.
[46] H. Fritzsche, et al., Phys. Rev. B 70 (2004) 214406.
[47] J.B. Laloe, et al., IEEE Trans. Magn. 42 (2006) 2933–2935.
[48] D. Schmitz, et al., J. Magn. Magn. Mater. 269 (2004) 89–94.
[49] M. Pannetier, T.D. Doan, F. Ott, S. Berger, N. Persat, C. Fermon, Europhys. Lett. 64 (2003) 524–528.
[50] S. Moyerman, et al., J. Appl. Phys. 99 (2006) 08r505.
[51] C. Schanzer, et al., Phys. B Condens. Matter 356 (2004) 46–50.
[52] Z.Y. Zhao, et al., Phys. Rev. B 71 (2005) 104417.
[53] M.R. Fitzsimmons, et al., Phys. Rev. Lett. 84 (2000) 3986–3989;
C. Leighton, et al., Phys. Rev. B 65 (2002) 064403/1–7;
M.R. Fitzsimmons, et al., Phys. Rev. B 65 (2002) 134436.
[54] M. Gierlings, et al., Phys. Rev. B 65 (2002) 092407/1–4.
[55] P. Blomqvist, et al., J. Appl. Phys. 96 (2004) 6523–6526.
[56] A. Paul, et al., Phys. Rev. B 73 (2006) 092410.
[57] S. Roy, et al., Phys. Rev. Lett. 95 (2005) 047201.

[58] G.P. Felcher, et al., Neutron News 5 (1994) 18–22.
[59] D.L. Nagy, et al., Phys. Rev. Lett. 88 (2002) 4.
[60] H. Lauter, et al., J. Magn. Magn. Mater. 258 (2003) 338;
V. Lauter-Pasyuk, et al., J. Magn. Magn. Mater. 226 (2001) 1694.
[61] A. Paul, et al., Phys. B Condens. Matter 356 (2005) 31.
[62] M. Gierlings, et al., Physica B 356 (2004) 36–40.
[63] A. Paul, et al., Physica B 356 (2005) 26–30.
[64] U. Rücker, E. Kentzinger, B. Toperverg, F. Ott, Th. Brückel, Appl. Phys. A 74 (2002) S607–S609.
[65] E. Kentzinger, U. Rucker, B. Toperverg, et al., Physica B 335 (2004) 89–94.
[66] S.V. Kozhevnikov, F. Ott, E. Kentzinger, A. Paul, Physica B 397 (2007) 68–70.
[67] F. Ott, A. Menelle, C. Fermon, P. Humbert, Physica B 283 (2000) 418–421.
[68] F. Ott, P. Humbert, C. Fermon, A. Menelle, Physica B 297 (2001) 189–193.
[69] S. Langridge, et al., Phys. Rev. B 74 (2006) 6.
[70] K. Theis-Brohl, Phys. B Condens. Matter 345 (2004) 161–168;
K. Theis-Brohl, et al., Phys. Rev. B 71 (2005) 4;
K. Theis-Brohl, et al., Physica B 356 (2005) 14.
[71] K. Theis-Brohl, et al., Phys. Rev. B 73 (2006) 14.
[72] E. Popova, et al., Europ. Phys. J. B 44 (2005) 491–500.
[73] K. Temst, et al., Europ. Phys. J. B 45 (2005) 261–266.
[74] K. Temst, et al., J. Magn. Magn. Mater. 304 (2006) 14–18.
[75] C. Fermon, et al., Physica B 267–268 (1999) 162–167.
[76] M. Pannetier, F. Ott, C. Fermon, Y. Samson, Physica B 335 (2003) 54–58.
[77] W. Szuszkiewicz, et al., J. Alloys Compounds 423 (2006) 172–175.
[78] Chang-Peng Li, et al., J. Appl. Phys. 100 (2006) 074318-25.
[79] T.D. Doan, et al., Physica B 335 (2003) 72–76;
T.-D. Doan, et al., Appl. Phys. A 74 (2002) S186–S188.
[80] V. Garcia, et al., Phys. Rev. Lett. 99 (2007) 117205.
[81] C. Dufour, K. Dumesnil, S. Soriano, et al., Phys. Rev. B 66 (9) (2002) 094428.
[82] K. Dumesnil, C. Dufour, P. Mangin, et al., Phys. Rev. B 60 (15) (1999) 10743–10746.
[83] A. Mougin, C. Dufour, K. Dumesnil, et al., Phys. Rev. B 59 (8) (1999) 5950–5959.
[84] A. Schreyer, et al., J. Appl. Phys. 87 (2000) 5443–5448.
[85] B. Hennion, et al., Phys. Rev. B 66 (2002) 224426;
B. Hennion, et al., J. Supercond. 16 (2003) 151–154.
[86] M. Bailleul, F. Ott, C. Fermon, Physica B 335 (1–4) (2003) 68–71.